

## **Force-matching-based parameterization of the Stillinger-Weber potential for thermal conduction in silicon**

Yongjin Lee and Gyeong S. Hwang\*

*Department of Chemical Engineering, University of Texas, Austin, Texas 78712, USA*

(Received 20 July 2011; revised manuscript received 21 November 2011; published 22 March 2012)

A force-matching method is employed to optimize the parameters of the Stillinger–Weber (SW) interatomic potential for calculation of the lattice thermal conductivity of silicon. The parameter fitting is based on first-principles density functional calculations of the restoring forces for atomic displacements. The thermal conductivities of bulk crystalline Si at 300–500 K estimated using nonequilibrium molecular dynamics with the modified parameter set show excellent agreement with existing experimental data. We also briefly discuss how the force-matching-based parameterization can provide the improved estimation of thermal conductivity, as compared to the original SW parameter set, through analysis of phonon density of states and phonon dispersion relations.



## **Force-matching-based parameterization of the Stillinger-Weber potential for thermal conduction in silicon**

Yongjin Lee and Gyeong S. Hwang<sup>\*</sup>

*Department of Chemical Engineering, University of Texas, Austin, Texas 78712, USA*

(Received 20 July 2011; revised manuscript received 21 November 2011; published 22 March 2012)

A force-matching method is employed to optimize the parameters of the Stillinger–Weber (SW) interatomic potential for calculation of the lattice thermal conductivity of silicon. The parameter fitting is based on first-principles density functional calculations of the restoring forces for atomic displacements. The thermal conductivities of bulk crystalline Si at 300–500 K estimated using nonequilibrium molecular dynamics with the modified parameter set show excellent agreement with existing experimental data. We also briefly discuss how the force-matching-based parameterization can provide the improved estimation of thermal conductivity, as compared to the original SW parameter set, through analysis of phonon density of states and phonon dispersion relations.



# Predicting Si Thermal Conductivity

300 K	(Tersoff <sup>13</sup> )	$235.7 \pm 7.5 \text{ Wm}^{-1}\text{K}^{-1}$
	experimental	130 W/mK
500 K	(SW <sup>8</sup> )	$119 \pm 40 \text{ Wm}^{-1}\text{K}^{-1}$
	experimental	$76.2 \text{ Wm}^{-1}\text{K}^{-1}$

# SW 2 and 3-Body

$$\Phi(r) = \sum_{i,j(i < j)} \Phi_2(r_i, r_j) + \sum_{i,j,k(i < j < k)} \Phi_3(r_i, r_j, r_k)$$

$$\Phi_2(r_{ij}) = \begin{cases} \varepsilon A (B r_{ij}^{-p} - r_{ij}^{-q}) \exp[1/(r_{ij} - a)], & r_{ij} < a \\ 0 & r_{ij} \geq a \end{cases} \quad (2)$$

$$\begin{aligned} \Phi_3(r_i, r_j, r_k) &= h(r_{ij}, r_{ik}, \theta_{ijk}) + h(r_{ij}, r_{jk}, \theta_{ijk}) \\ &\quad + h(r_{ki}, r_{kj}, \theta_{ikj}); \\ h(r_{ij}, r_{ik}, \theta_{jik}) &= \varepsilon \lambda \exp[\gamma/(r_{ij} - a) \\ &\quad + \gamma/(r_{ik} - a)] (\cos \theta_{jik} + 1/3)^2 \end{aligned} \quad (3)$$



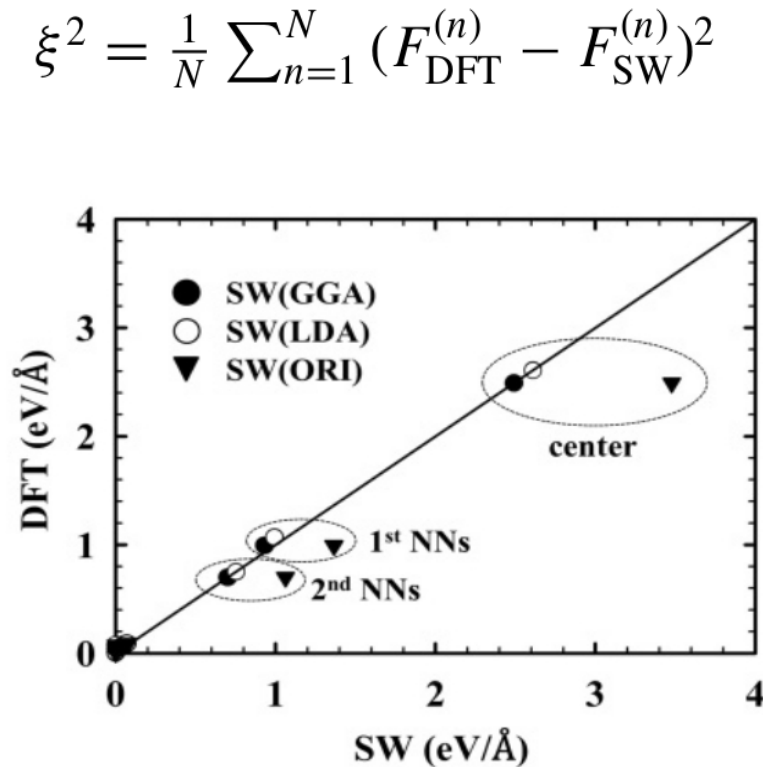
# SW Original Fitting

In the original study, the seven parameters ( $A$ ,  $B$ ,  $p$ ,  $q$ ,  $a$ ,  $\lambda$ , and  $\gamma$ ) were adjusted to give a diamond lattice structure in the solid state and fit molecular dynamics simulation results to experimental observations for melting temperature and liquid structure. In addition, the values of  $\sigma$  and  $\varepsilon$  were chosen to match the observed lattice constant and atomization energy of crystalline Si at 0 K, respectively. Although the SW potential overall gives a fairly realistic description of crystalline Si, as stated earlier, the thermal conductivities calculated based on the original SW parameters<sup>18</sup> tend to be overestimated. Since



# Force-Matching Method

The DFT force data for parameter optimization were obtained by displacing one atom in the  $x$ ,  $y$ , and  $z$  directions by 0.2 Å; the magnitude of the displacements was carefully determined from test calculations with different values which were greater than the mean atomic displacement of about 0.077 Å in  $c$ -Si at 300 K.<sup>28</sup> The restoring forces acting on the displaced atom and its four first- and 12 second-nearest neighbors were considered to be matched in the SW parameter adjustments. On the third-nearest neighbors and beyond, the forces due to the center-atom displacement are negligible ( $<0.01$  eV/Å in the absolute value). The optimal values for



$$F_i = - \frac{\partial V}{\partial u_i}$$

$$= -\Pi_i - \sum_j \Phi_{ij} u_j - \frac{1}{2} \sum_{jk} \Psi_{ijk} u_j u_k - \frac{1}{3!} \sum_{jkl} \chi_{ijkl} u_j u_k u_l$$

FIG. 1. Discrepancies between DFT and SW predictions for the restoring forces acting on the displaced atom (center) and its four first- (1<sup>st</sup> NNs) and 12 second-nearest neighbors (2<sup>nd</sup> NNs).

# Re-Fit SW

## B. Parameter optimization using a force-matching method

To improve the description of lattice dynamics, using a force-matching method,<sup>29</sup> we adjusted three SW parameters ( $\sigma$ ,  $\varepsilon$ , and  $\lambda$ ) to fit DFT results for both the lattice spacing and the lattice restoring forces arising from local lattice distortions. The values of  $\sigma$  were chosen to match the LDA/GGA lattice constants for the Si diamond structure. In the SW potential,  $\varepsilon A$  and  $\varepsilon \lambda$  determine the relative strength between the two- and three-body interactions. Since  $A$  is preset,  $\varepsilon$  and  $\lambda$  were tuned to fit the DFT restoring forces.

TABLE I. Parameters of the Stillinger–Weber interatomic potential in Eqs. (2) and (3); original<sup>19</sup> [SW(ORI)] and modified values based on fit to GGA [SW(GGA)] and LDA [SW(LDA)] calculations (this paper).

	$\sigma$	$\varepsilon$ (eV)	$\lambda$	
SW(ORI)	2.0951	2.1683	21	$A = 7.049556277$
SW(GGA)	2.1051937	1.41992	29.5304	$B = 0.6022245584$
SW(LDA)	2.0780213	1.49662	26.4091	$\gamma = 1.2, a = 1.8$ $p = 4.0, q = 0.0$

predicted GGA (LDA) Si lattice constants  
 $5.4571$  ( $5.3865$ ) Å





# NEMD Simulation

109.142, and 130.97, to 174.627 nm (corresponding to 120, 160, 200, 240, and 320 shells, respectively).

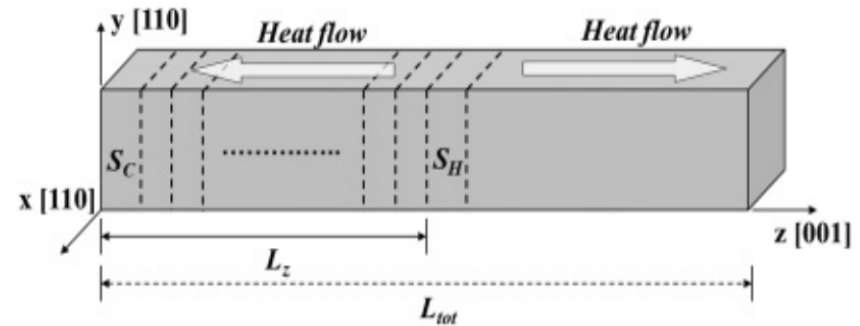
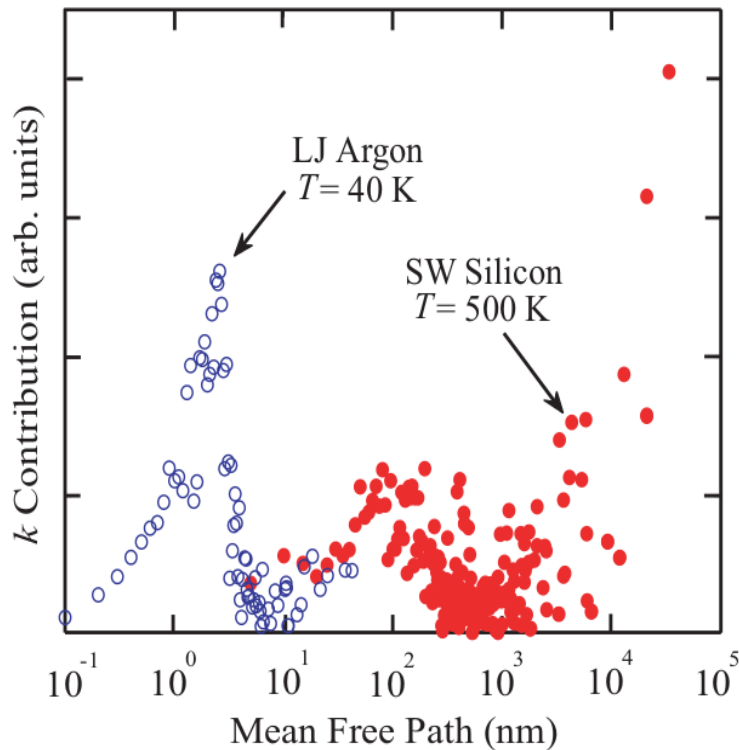


FIG. 2. Schematic illustration of a rectangular-shaped simulation domain with periodic boundary conditions imposed in the  $x$ ,  $y$ , and  $z$  directions, where heat conduction occurs in the  $z$  (or [100]) direction. The simulation domain is axially divided into a number of thin shells (each of which contains 400 atoms) while having heat source ( $S_H$ ) and heat sink ( $S_C$ ) layers, as indicated.



# Finite-Size Extrapolation

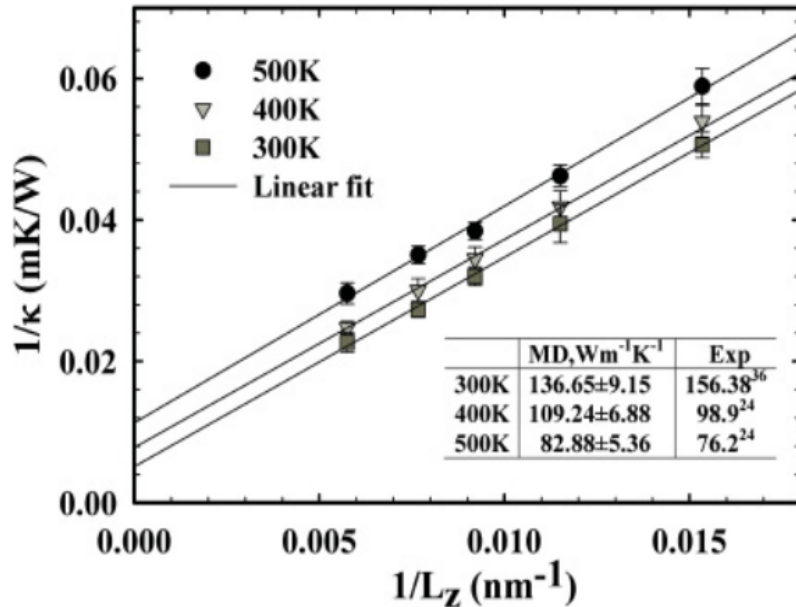
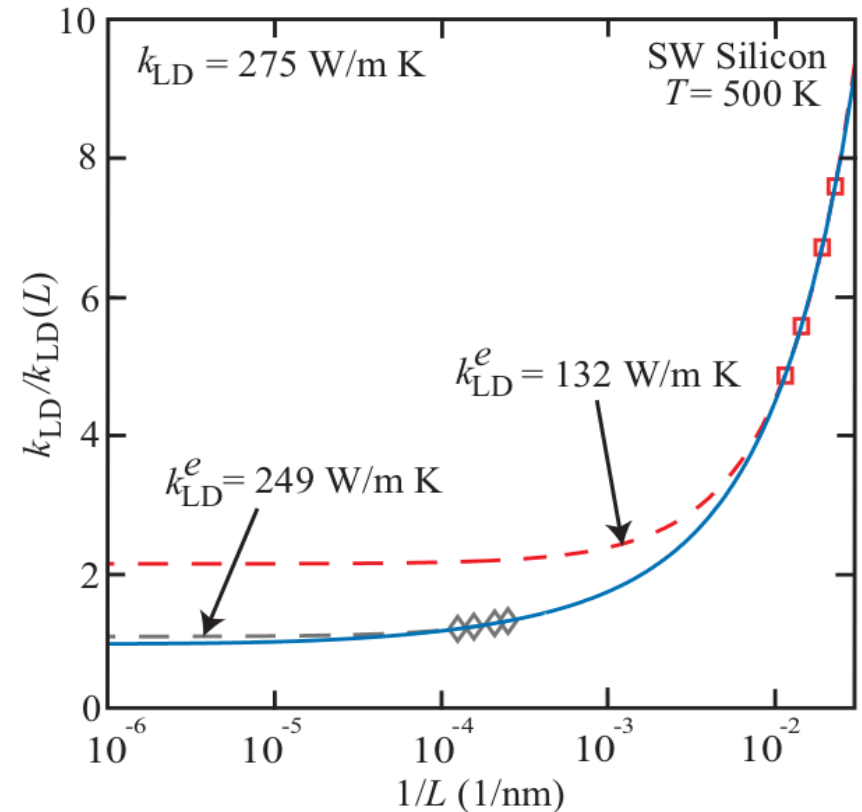
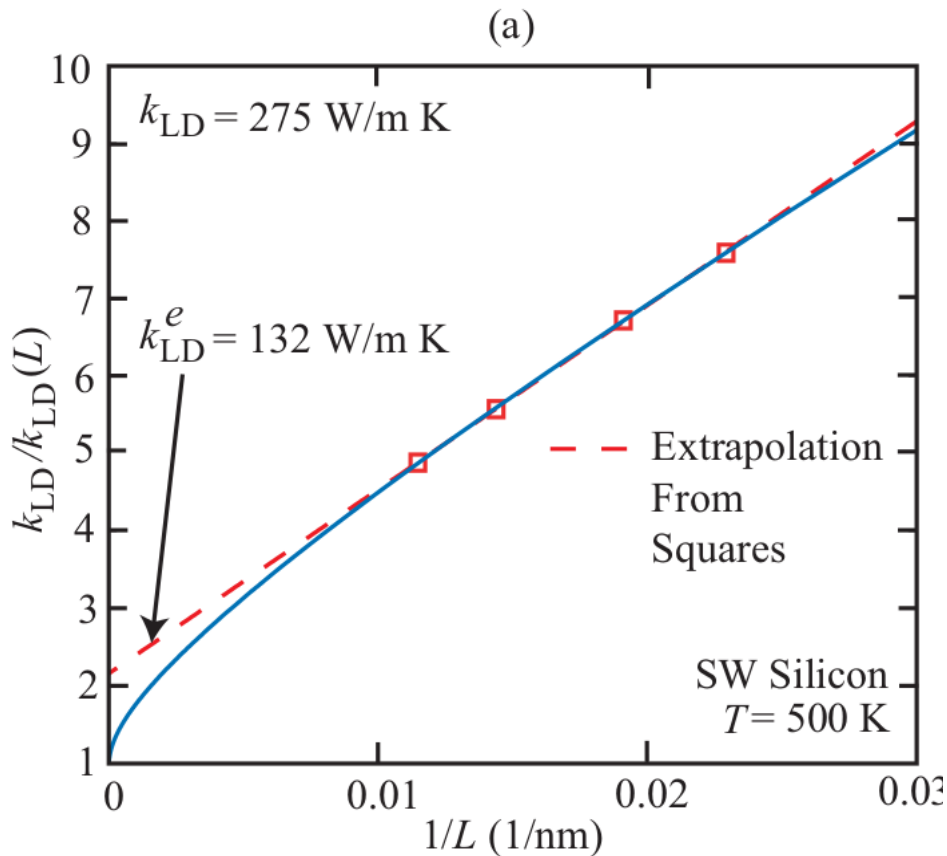


FIG. 3. Thermal resistivity ( $1/\kappa$ , after quantum corrections) for *c*-Si as a function of simulation cell length at three different temperatures as indicated; for each set, the linear line indicates the best-fit linear regression. Here,  $L_z$  is the distance between the heat source and heat sink centers, which is half of the total simulation domain length ( $L_{\text{tot}}$ ; see Fig. 2). The inset summarizes the calculated thermal conductivities of *c*-Si based on SW(GGA), with the available experimental values (Refs. 24 and 36) for comparison.

Note that, according to Schelling *et al.*,<sup>8</sup> the relationship between size-dependent thermal conductivity and simulation domain length ( $L_{\text{tot}} = 2L_z$ , where  $L_z$  is the distance between the heat source and heat sink centers, which is half of the total simulation domain length) is given by:  $\frac{1}{\kappa} \propto (\frac{1}{l_{\infty}} + \frac{2}{L_z})$ , where  $l_{\infty}$  is the phonon mean free path for the infinite system. We expect that the linear extrapolation approach

	MD, Wm <sup>-1</sup> K <sup>-1</sup>	Exp
300K	136.65±9.15	156.38 <sup>36</sup>
400K	109.24±6.88	98.9 <sup>24</sup>
500K	82.88±5.36	76.2 <sup>24</sup>

# Finite-Size Extrapolation?



PHYSICAL REVIEW B 81, 214305 (2010)

# Quantum Corrections?

## Assessing the applicability of quantum corrections to classical thermal conductivity predictions

J. E. Turney,<sup>1</sup> A. J. H. McGaughey,<sup>1,\*</sup> and C. H. Amon<sup>1,2</sup>

<sup>1</sup>*Department of Mechanical Engineering, Carnegie Mellon University, Pittsburgh, Pennsylvania 15213, USA*

<sup>2</sup>*Department of Mechanical and Industrial Engineering, University of Toronto, Toronto, Ontario, Canada M5S 3G8*

(Received 3 March 2009; revised manuscript received 29 May 2009; published 25 June 2009)

$$\sum_{\kappa, \nu}^{N, 3n} E^C \left( \begin{matrix} \kappa \\ \nu \end{matrix} \right) = \sum_{\kappa, \nu}^{N, 3n} E^Q \left( \begin{matrix} \kappa \\ \nu \end{matrix} \right), \quad k^Q = k^C \frac{dT^C}{dT^Q},$$

We have assessed the validity of the commonly used QCs for thermal conductivity [Eqs. (2) and (4)] by using harmonic and anharmonic LD calculations to self-consistently predict the quantum and classical thermal conductivities of SW silicon. Applying the QCs to the classical predictions, with or without the ZP energy, does not bring them into better agreement with the quantum predictions compared to the uncorrected classical values above temperatures of 200 K (see Fig. 1). When neglecting the ZP energy, the quantum-

Quantum  
Corrected

	MD, Wm <sup>-1</sup> K <sup>-1</sup>	Exp
300K	136.65±9.15	156.38 <sup>36</sup>
400K	109.24±6.88	98.9 <sup>24</sup>
500K	82.88±5.36	76.2 <sup>24</sup>



# Si Dispersion

$$\left[ f\left(\frac{\kappa'}{\nu'}\right) + f\left(\frac{\kappa''}{\nu''}\right) + 1 \right] \left[ \delta\left(\omega\left(\frac{\kappa}{\nu}\right) - \omega\left(\frac{\kappa'}{\nu'}\right) - \omega\left(\frac{\kappa''}{\nu''}\right)\right) \right]$$

according to the kinetic theory,  $\kappa \propto \nu C_v l$ , where  $\nu$  is the group velocity of acoustic branches,  $C_v$  is the specific heat of phonons per unit volume, and  $l$  is the mean free path of phonons.<sup>24</sup>

ALD 3-phonon

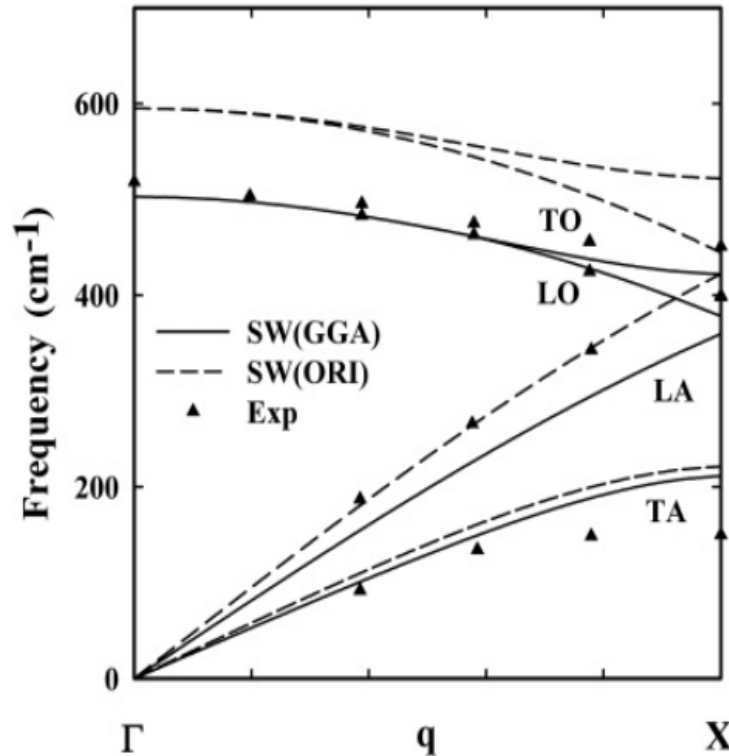


FIG. 5. Phonon dispersion for *c*-Si along high-symmetry directions. The SW(GGA) and SW(ORI)-based calculations were performed using the GULP (General Utility Lattice Program) computer program (Ref. 39). The solid and dashed lines correspond to the modified [SW(GGA)] and original [SW(ORI)] parameter sets, respectively. Triangles indicate experimental data from Ref. 38.

# Harmonic Frequencies

- No carrier-level analysis

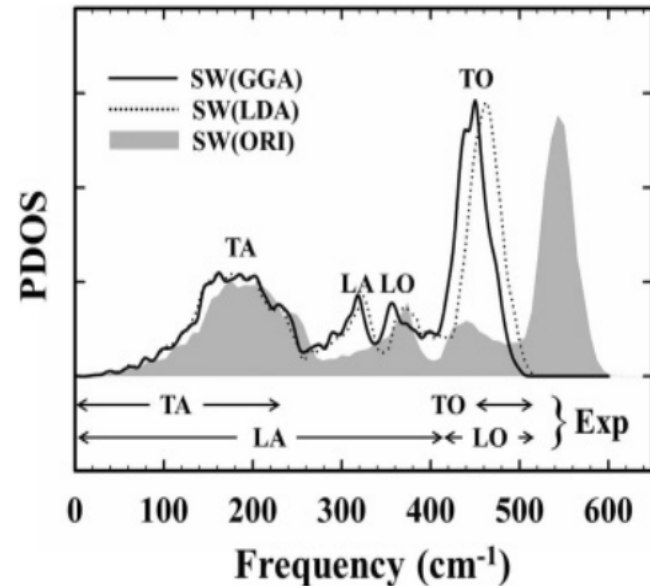


FIG. 4. Phonon density of states (PDOS) calculated based on different sets of SW parameters, as indicated; each of which consists of four longitudinal acoustic (LA), transverse acoustic (TA), longitudinal optical (LO), and transverse optical (TO) branches. For comparison, the relative positions of the four phonon branches extracted from experimental phonon-dispersion relations (Refs. [37](#) and [38](#)) are also presented, as indicated.